An Estimation Method of High-order LC Circuits in Power Electronic Converters

Bo, Yao; Peng, Yingzhou; Zhang, Yichi; Wang, Haoran; Wang, Huai

Published in:
I E E E Transactions on Industrial Electronics

DOI (link to publication from Publisher):
10.1109/TIE.2023.3285917

Publication date:
2024

Document Version
Accepted author manuscript, peer reviewed version

An Estimation Method of High-order LC Circuits in Power Electronic Converters

Bo Yao, *Student Member, IEEE,* Yingzhou Peng, *Member, IEEE,* Yichi Zhang, *Student Member, IEEE,* Haoran Wang, *Member, IEEE,* and Huai Wang, *Senior Member, IEEE*

***Abstract*—This paper proposes a parameter estimation method for high-order LC circuits conducted during the power-OFF of power electronic converters. It is based on a battery-powered compact signal injection unit and a circuit modeling method to estimate the LC circuit parameters. The proposed method aims for LC component condition monitoring in applications with routine-based maintenance or frequent ON/OFF operation (e.g., wind power, photovoltaic, traction systems). Compared to LCR meters and impedance analyzers, the proposed method has a significantly lower implementation cost and does not require disassembly of components. Moreover, it is a converter-level method in which the signal injection unit only needs to connect the converter inputs or outputs. Compared to power-ON LC parameter estimation methods, the proposed one is non-invasive without adding any hardware or software algorithm that may introduce new risks to converter operation. This method can handle the converters with high-order LC structures (e.g., 2^{nd} to 4^{th}-order) in converter power-OFF state, which has not been achieved by existing power-OFF solutions. Therefore, the proposed method is promising for the specific applications of interest mentioned above. The parameter estimation algorithm and signal injection unit design are presented. The experimental results indicate that the estimation errors of the 2^{nd}-order equivalent circuit, 3^{rd}-order equivalent circuit, and 4^{th}-order equivalent circuit are lower than 1.6%, 2.5%, and 3%, respectively. The estimated LC parameters can be further used as inputs for operation optimization or condition monitoring of the converters.**

***Index Terms*—Estimation method, signal injection, non-invasive, LC parameters, high order circuits, converters.**

I. Introduction

THE passive component parameters are critical to the performance optimization and reliability evaluation of power electronic converters [1] [2]. Their values are affected by tolerances, operational and environmental conditions. Hence, the determination of these parameter values cannot rely on datasheet information and requires online measurement or estimation [3]–[5]. Parameter estimation methods can be mainly divided into the component off-line characterization, converter power-OFF, and converter power-ON [6].

The estimation for the component off-line characterization is a method where the individual components are evaluated independently [7]–[10]. One way is to use the LCR meters and the impedance analyzers, which can test the LC circuits with 2^{nd} and 3^{rd} -order, respectively [7], but it requires the huge volume and high cost equipment. Another method is that measuring the parameters of 2^{nd}-order circuits by step response of the injected signal, which has lower measurement costs than impedance analyzers [8]. In addition, a method based on the resonant frequency of the acquired signals to estimate the parameters is proposed in [9] [10], which is also only suitable for individual components with 2^{nd}-order circuits.

The estimation methods for converter power-ON do not require the converter with a power-OFF state. A 1^{st}-order capacitor parameter estimation method is proposed in AC/DC/AC converters with low-frequency signals to be injected into the DC-link voltage [11], which need to inject additional signals in the operating converters. In single phase inverter systems, a 1^{st}-order capacitance estimation method is given in [12], but it needs to intrude into control system to calculate capacitor current. Ref. [13] gives a 1^{st}-order DC-link parameter estimation method in aerospace drive systems However, this method needs to additional current sensor to deal with the AC component of the modulation signals. Therefore, additional sensors or programs are usually required to intrude into the original circuit structure in converter power-ON state. Additionally, the evaluated response signals are also affected by the converter operation dynamics.

The parameter estimation for converter power-OFF has the advantage of low-risk testing and strong noise interference tolerance capability. Meanwhile, it is not necessary to have continuous parameter estimation for condition monitoring as the LC parameter shifts due to component long-term degradation is a slow process [14]. The estimation methods for converter power-OFF can be implemented on-site in practical applications that have a power outage maintenance program and a convenient interface for the signal injection, such as systems of tractions, electric vehicles, and solar photovoltaics. Ref. [15] gives the method of estimating the 2^{nd}-order LC parameters through the discharge circuit composed of LC filters and braking resistors in traction systems. This method needs to collect the current on the branch of the LC filter, and additional current sensors are still limited. In [16], the 1^{st}-order capacitance can be estimated by injecting low-frequency harmonic currents into the grid when the photovoltaic system is shut down, but it requires the intrusive connection of blocking diodes in the photovoltaic panels. A 1^{st}-order capacitance estimation method based on component voltage and current in the electric vehicle converters is given in [17],

Manuscript received xx; revised xx; accepted xx. (*Corresponding author: Yingzhou Peng.*)

B. Yao, Y. Zhang, and H. Wang are with the Department of Energy, Aalborg University, 9220 Aalborg, Denmark (e-mail:ybo@energy.aau.dk, yzhang@energy.aau.dk, and hwa@energy.aau.dk).

Y. Peng is with the School of Electrical Engineering, Hunan University, Hunan, China (e-mail:yzpeng@hnu.edu.cn).

H. Wang is with the Three Gorges Intelligent Industrial Control Technology Co., Ltd. China (e-mail:wang_haoran@ctg.com.cn).

TABLE I
COMPARISON OF LC PARAMETER ESTIMATION METHODS IN CONVERTER SYSTEMS.

	Ref.	Working principle	Advantage		Limitation		Circuit orders	Exp. error
Component off-line	[7]	Measurement by frequency sweeping	1. Not interface with converters operation 2. No risk for the converters	3. High measurement accuracy	1. Require disassembly of components	2. Expensive and huge impedance analyzer	3rd order	1%
	[8]	Measurement by step response of the injected signal		3. Lower measurement costs than impedance analyzers		2. Still requires extensive measurement equipment and circuits	2nd order	4.9%
	[9] [10]	Measurement by the resonant frequency of the components					2nd order	2.1%
Converter power-ON	[11]	Monitoring by injecting low-frequency signal in DC link	1. Can evaluate in the power-ON state for converters	2. Consider the effect of the DC-link voltage on the output current	1. Require interface with converters operation 2. Results are affected by converters operation	3. Need to inject additional signals in the operating circuit	1st order	5%
	[12]	Monitoring by DC-link voltage and estimated capacitor current		2. No need for additional current and voltage sensors		3. Need to intrude into control system to calculate capacitor current	1st order	2.6%
	[13]	Monitoring by impedance calculation of capacitor parameters		2. Condition monitoring system independent of drive operation		3. Require the additional current sensor	1st order	4.3%
Converter power-OFF	[15]	Estimation by the discharge circuit of LC filters	1. Not require interface with converters operation 2. Results are not affected by converters operation	3. Low sampling frequency requirement of the measured signal	Need to additional high-level current sensors for the LC filter branch.		2nd order	2.5%
	[16]	Estimation by injection of low-frequency harmonic current in grid		3. No need for additional current and voltage sensors	Require intrusive connection of blocking diodes in the PV panel		1st order	1.5%
	[17]	Parameters estimation based on component voltage and current			Require intrusion into the controller to collect current and voltage signals		1st order	1.9%
	[18] [19]	Estimation by impedance calculation of equivalent circuits			Require intrusion into the original control system for setting the constant duty cycle		2nd order	5.1%
	[20]	Estimation by introducing LC resonance			Need to intrusion into the original control system to turn on the IGBT of the power module		2nd order	2.1%

but this method requires intrusion into the controller to collect current and voltage signals in converter power-OFF state. In [18] [19], the 2^{nd}-order RC parameters can be estimated at a specific controlled unipolar PWM operation mode in adjustable-speed drive systems. A 2^{nd}-order LC parameters estimation method in voltage source inverter systems is given in [20], which introduces an LC resonance when the system is not in operation. However, the estimation methods in [18]–[20] require modifying the original control system to turn on the switch for the converters.

The working principle, advantages, and limitations of the existing methods are summarized in Table I. Due to the need to disassemble the converter in off-line component methods, it has limitations in those already assembled converters in component off-line state [7]–[10]. In converter power-ON state, existing methods require additional sensors or programs to intrude into the original circuit, and the estimation results are affected by converter operation [11]–[13]. Since the power-OFF state has the advantages of not requiring an interface with the converter operation and the results are not affected by the converter operation, this paper focuses on the converter power-OFF state. Overall, there are still two challenges for the existing converter power-OFF estimation methods that have not been addressed: how to perform parameter estimation without modifying existing hardware and control systems, thus minimizing the risk to the converter from the estimation process [6]. Moreover, those estimation methods are just suitable for 1^{st}-order [16], [17] and 2^{nd}-order [15], [18]–[20] circuit networks. Nevertheless, the widespread use of DC-link and AC side filters in the converters introduces high-order circuits with more components, such as filter inductors and AC capacitors on the AC side of the converter systems [21] [22]. The high-order circuits increase the difficulty of parameter estimation dramatically and has not been fully investigated. Based on the above challenges, this paper proposes a non-invasive parameter estimation method for high-order LC circuits with the following advantage: 1) it does not need to modify and intrusion into the control and circuit of the converter to be monitored; 2) it can handle the converters with high-order LC structures (e.g., 2^{nd} to 4^{th}-order); 3) it provides a plug-and-play carry-on prototype with a low cost and a small volume. Since the signal injection does impose a potential risk to the converter and the converter operation also affects the measured response signals. This paper limits its scope to a case study for the converter power-OFF scenario.

The paper is organized as follows: Section II presents the mechanism modeling; Section III gives the estimation algorithm; Experiments and results are shown in Section IV; Discussions of the testing setup are given in Section V, followed by the conclusions.

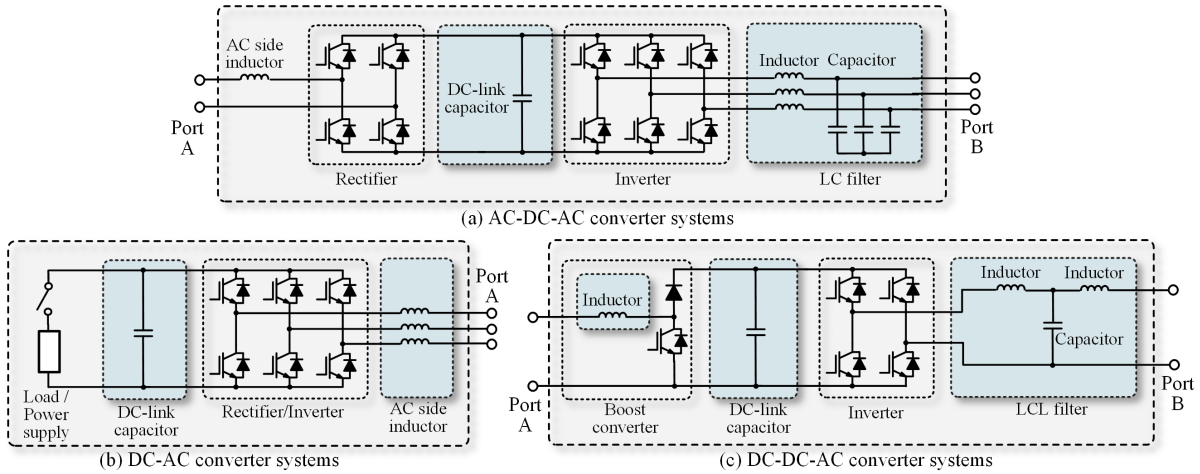

Fig. 1. Three different power electronic converter configurations. (The single-phase and three-phase converters are interchangeable in these three topologies; A and B represent different interface ports for the signal injection.)

II. Description and Modeling of the Power Converters of Interest

A. Power converters description of interest

The parameter estimation of converter power-OFF is suitable for applications, which have a power-OFF maintenance program and a convenient interface for the signal injection, and three applicable structures for power electronic converters are shown in Fig. 1. The AC-DC-AC systems in Fig. 1. (a) can be applied to wind power and traction systems [21] [23]. The DC-AC systems in Fig. 1. (b) are widely used in electric vehicle systems, industrial and household appliances [24] [25]. The DC-DC-AC systems in Fig. 1. (c) are suitable for solar photovoltaic and microgrid systems [22] [26]. It is worth mentioning that the single-phase and three-phase converters are interchangeable in these three topologies. This paper uses the circuit structure in its most complete form as an example to illustrate the proposed method, and it is reasonable to derive that the proposed method is also applicable to many other converter topologies.

In the converter power-OFF conditions, the IGBTs in the converter are turned off, and its current signal can only flow in one direction through the reverse diode. Its equivalent LC circuit network is shown in Fig. 2, which can be divided into 2^{nd}-order, 3^{rd}-order, and 4^{th}-order circuits according to the different converter structures. Specifically, the 2^{nd}-order LC circuit network in Fig. 2(a) corresponds to the power-OFF circuit from Port A in Fig.1(a), Port A in Fig. 1 (b), and Port A in Fig. 1 (c). The 3^{rd}-order LC circuit network in Fig. 2(b) corresponds to the power-OFF circuit from Port B in Fig. 1(a). The 4^{th}-order LC circuit network in Fig. 2(c) corresponds to the power-OFF circuit from Port B in Fig. 1(c). If the port of the tested circuit is the three-phase terminal, the signal can be injected from any two-phase terminal. The method provided in this paper adopts a DC voltage source U_{in} and a voltage divider resistance R_s. The output voltage value in the DC voltage source is H, and the flow direction of the injected signal of the DC voltage source is unidirectional.

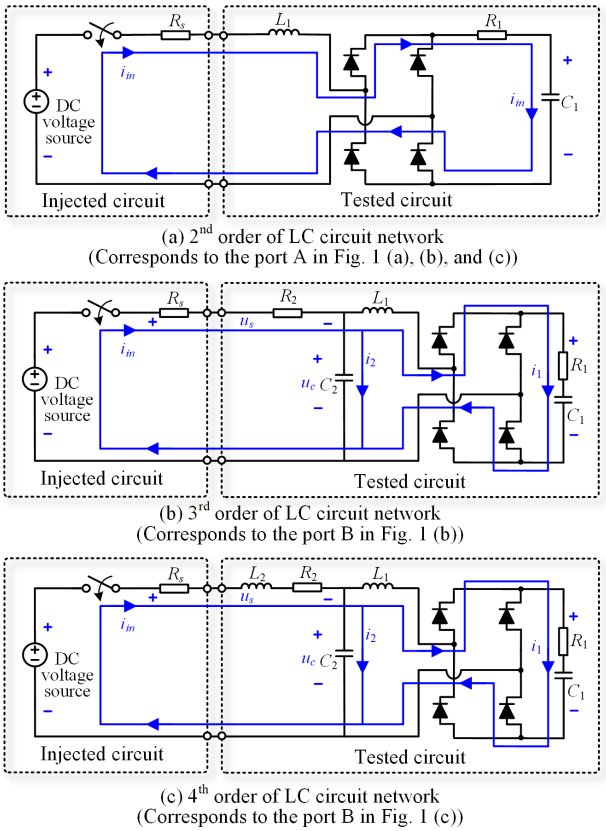

Fig. 2. Physical systems represented by different order of LC circuit network. (L_1, L_2, C_1 and C_2 are evaluated LC parameters; R_1 and R_2 represent parasitic resistances.)

B. Converter power-OFF circuit networks modeling

1) 2^{nd}-order LC circuit network: Fig. 2(a) shows the physical system for the test circuit without AC filter capacitors on the AC side (such as the injection from port A in Fig. 1(a), (b), and (c)). In this circuit, R_1 represents the parasitic resistance in the test circuit, including the equivalent line resistance, the equivalent series resistance (ESR) of the filter inductors, and the ESR of the DC-link capacitor. L_1 and C_1 represent the inductance of the filter inductors, and the capacitance of the DC-link capacitor, respectively.

Therefore, the state-response equation of this LC circuit network can be expressed as:

$$U_{in} = L_1 \frac{di_{in}}{dt} + (R_1 + R_s) i_{in} + \frac{1}{C_1} \int i_{in} dt \tag{1}$$

where i_{in} is the input current of the testing circuit.

Further, (1) can be expressed into a 2^{nd}-order differential equation:

$$\begin{cases} L_1 \dfrac{d^2 i_{in}}{d^2 t} + (R_1 + R_s) \dfrac{di_{in}}{dt} + \dfrac{1}{C_1} i_{in} = 0 \\ i_{in}\,(0_+) = 0 \\ \dfrac{di_{in}}{dt}\,(0_+) = \dfrac{H}{L_1} \end{cases} \tag{2}$$

According to the solution of the 2^{nd}-order differential equation, the input current i_{in} can be given as:

$$\begin{cases} i_{in} = H \dfrac{e^{\frac{R - \sqrt{R^2 - \frac{4L_1}{C_1}}}{-2L_1} t} - e^{\frac{R + \sqrt{R^2 - \frac{4L_1}{C_1}}}{-2L_1} t}}{\sqrt{R^2 - \frac{4L_1}{C_1}}} \\ R = R_1 + R_s \end{cases} \tag{3}$$

The output current is concurrently affected by the LC parameters of inductance and capacitance in (3). In the next part, the influence of different circuit parameter changes on the input current is specifically considered.

2) 3^{rd}-order LC circuit network: Fig. 2(b) shows the physical system with an LC filter on the AC side (such as the injection from port B in Fig. 1(a)). In this circuit, R_1 represents the parasitic resistance in one branch, including the equivalent line resistance from the AC inductor to the DC link, the ESR of the filter inductors, and the ESR of the DC-link capacitor. R_2 represents the parasitic resistance from the output terminal to the AC inductor in another branch. C_1, L_1 and C_2 represent the capacitance of the DC-link capacitor, the inductance of the AC filter inductor, and the capacitance of the AC filter capacitor, respectively.

The state-response equation of this LC circuit network can be expressed as:

$$\begin{cases} U_{in} = u_s + u_c \\ u_s = (R_2 + R_s)\,(i_1 + i_2) \\ u_c = L_1 \dfrac{di_1}{dt} + R_1 i_1 + \dfrac{1}{C_1} \int i_1 dt = \dfrac{1}{C_2} \int i_2 dt \end{cases} \tag{4}$$

where u_s and u_c represent the voltages of R_s and R_2, and the voltage of C_2, respectively. i_1 and i_2 represent the currents on the two branches.

Further (4) can be expressed into a 3^{rd}-order differential equation:

$$\begin{cases} (R_2 + R_s) C_2 L_1 \dfrac{d^3 i_1}{d^3 t} + ((R_2 + R_s) C_2 R_1 + L_1) \dfrac{d^2 i_1}{d^2 t} \\ + \left((R_2 + R_s)(\dfrac{C_2}{C_1} + 1) + R_1 \right) \dfrac{di_1}{dt} + \dfrac{1}{C_1} i_1 = 0 \\ i_1(0+) = 0 \quad \dfrac{di_1}{dt}(0+) = 0 \\ \dfrac{d^2 i_1}{d^2 t}(0+) = \dfrac{H}{(R_s + R_2)\, C_2 L_1} \end{cases} \tag{5}$$

According to the solution of the 3^{rd}-order differential equation, the current of one parallel branch i_1 can be given. 3^{rd}-order differential equations can be calculated by the $dsolve$ solver in Matlab [27].

Thereby the input current i_{in} is obtained as:

$$\begin{cases} i_2 = C_2 L_1 \dfrac{d^2 i_1}{d^2 t} + C_2 R_1 \dfrac{di_1}{dt} + \dfrac{C_2}{C_1} i_1 \\ i_{in} = i_1 + i_2 \end{cases} \tag{6}$$

3) 4^{th}-order LC circuit network: Fig. 2(c) shows the physical system with an LCL filter on the AC side (such as injection from port B in Fig. 1(c)). Different from Fig. 2(b), L_1 and L_2 represent two inductances of the LCL filter in this circuit. The state-response equation of this LC circuit network can be expressed as:

$$\begin{cases} U_{in} = u_s + u_c \\ u_s = L_2 \dfrac{d\,(i_1 + i_2)}{dt} + (R_2 + R_s)\,(i_1 + i_2) \\ u_c = L_1 \dfrac{di_1}{dt} + R_1 i_1 + \dfrac{1}{C_1} \int i_1 dt = \dfrac{1}{C_2} \int i_2 dt \end{cases} \tag{7}$$

where u_s represents the voltage of the branch of R_s, L_2, and R_2. u_c represents the branch of C_2.

(7) can be organized into a 4^{th}-order differential equation:

$$\begin{cases} L_1 C_2 L_2 \dfrac{d^4 i_1}{d^4 t} + ((R_2 + R_s) C_2 L_1 + L_2 C_2 R_1) \dfrac{d^3 i_1}{d^3 t} + \\ \left((R_2 + R_s) C_2 R_1 + L_2 \dfrac{C_2}{C_1} + L_1 + L_2 \right) \dfrac{d^2 i_1}{d^2 t} \\ + \left((R_2 + R_s)(\dfrac{C_2}{C_1} + 1) + R_1 \right) \dfrac{di_1}{dt} + \dfrac{1}{C_1} i_1 = 0 \\ i_1(0+) = 0 \quad \dfrac{di_1}{dt}(0+) = 0 \\ \dfrac{d^2 i_1}{d^2 t}(0+) = 0 \quad \dfrac{d^3 i_1}{d^3 t}(0+) = \dfrac{H}{C_2 L_1 L_2} \end{cases} \tag{8}$$

According to the solution of the 4^{th}-order differential equation, the current of one parallel branch i_1 can be given. 4^{th}-order differential equations also can be calculated by the $dsolve$ solver in Matlab [27]. Similarly, according to (7), the analytical expressions of the current in the other parallel branch i_1 and the input current i_{in} can be obtained.

C. Calculation results of circuit modeling

This part shows the calculation results of circuit modeling with different parameter values. The output voltage H of the injected DC source is set to 24V (safe voltage), and the voltage dividing resistor R_s is set to 3 Ω. The setup of R_s is discussed in Section V.

According to the analytical solution for 4^{th}-order differential equation, Fig. 3 shows a parameter variation example with the 4^{th}-order LC circuit network. In this case, the capacitance and inductance are set to vary from 100% to 80% and the resistance from 100% to 200%. From the results, even if there are 6 potential parameters to change, the change characteristics of the input current corresponding to different parameter changes are different. Therefore, it provides a way to use the input current change to evaluate the parameter change in the test circuit.

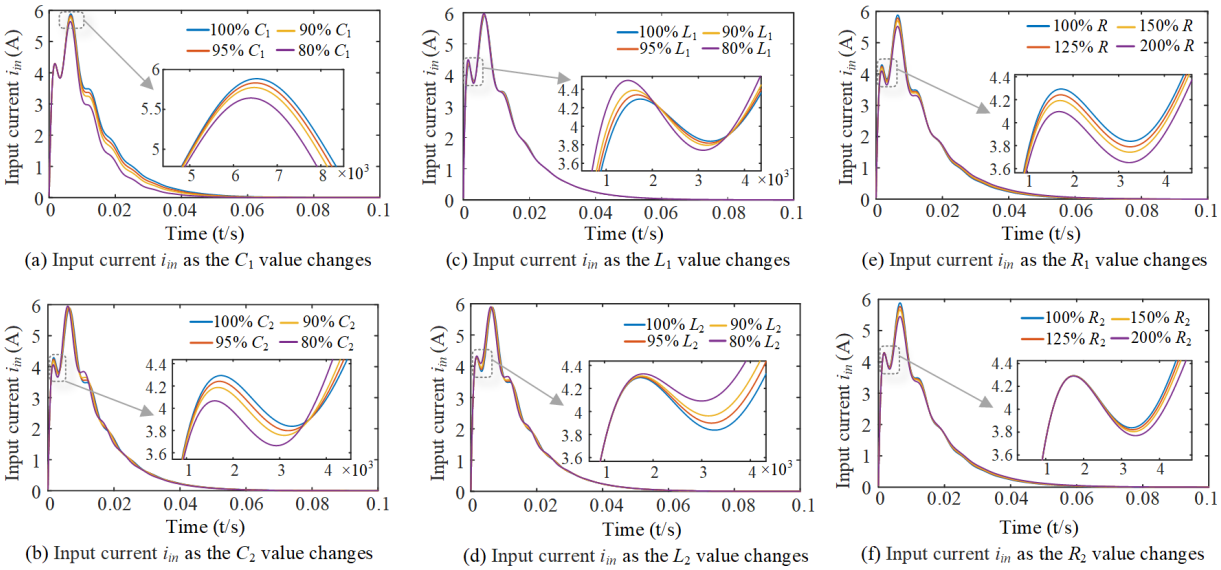

(a) Input current i_{in} as the C_1 value changes
(c) Input current i_{in} as the L_1 value changes
(e) Input current i_{in} as the R_1 value changes
(b) Input current i_{in} as the C_2 value changes
(d) Input current i_{in} as the L_2 value changes
(f) Input current i_{in} as the R_2 value changes

Fig. 3. Input current under different parameter changes based on mathematical models (4^{th}-order circuit). (Voltage dividing resistance R_s =3 Ω, test circuit capacitance C_1=450 μF, C_2=3.2 mF; test circuit inductance L_1=4 mH, L_2=4 mH; test circuit equivalent series resistance R_1 =300 $m\Omega$, R_2 =300 $m\Omega$.)

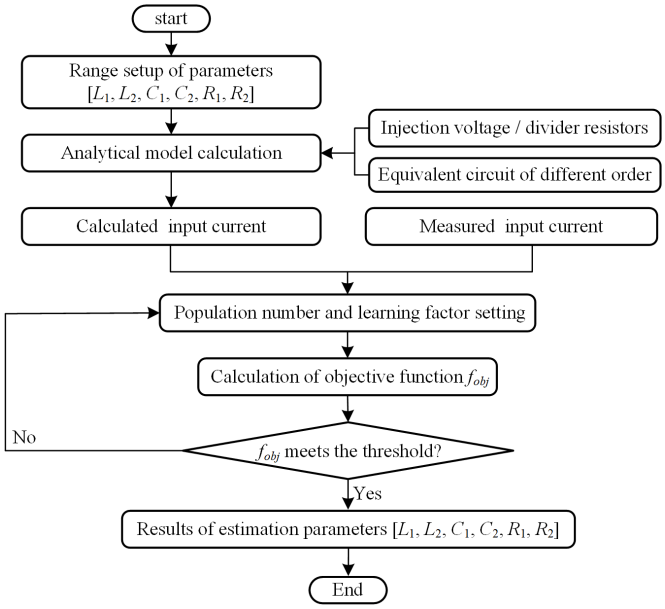

Fig. 4. Flowchart of the parameter estimation process.

III. Algorithm Used for Obtaining LC Parameters

As mentioned in the previous section, the analytical expression of input current i_{in} contains nonlinear complex components, in which the resistance, inductance, and capacitance of different branches are independent variables. The swarm intelligence computing algorithm, such as BA (Bat Algorithm) is a global optimization algorithm [28] [29]. It can be used to find the optimal solution for the undetermined parameters, which is suitable for analyzing the value of the undetermined parameter of this test circuit.

Fig. 4 shows the flowchart of the estimation process. Firstly, the ranges of the component parameters are set, including evaluated LC parameters L_1, L_2, C_1 and C_2, and parasitic resistances R_1 and R_2. For applications in which the component part numbers and rated specifications are known, the ranges can be reasonably assumed by considering the deviations due to tolerances, parameter shifts due to varying operating points and degradation, and conservative margins. Next, the calculated value of the input current can be obtained according to the analytical models proposed in Section II.

To implement BA, the first step is to set the population size and learning factor, whose values can be assumed empirically and updated in follow-up calculations. Next, an objective function needs to be constructed [30]. In this paper, the objective function is as follows:

$$f_{obj} = \sum_{i=0}^{t} \left| \frac{i_{cal(t)} - i_{test(t)}}{i_{test(t)}} \right| \tag{9}$$

where $i_{cal(t)}$ and $i_{test(t)}$ represent the calculated input current and measured input current during the testing time, respectively.

The calculation results of the input current corresponding to different parameter values in the setting range are compared with the actual test results and iterative training. When the result of f_{obj} is the minimum, the corresponding parameters are output, which is the optimal solution. If the result is below a threshold, the corresponding component parameters used for the calculation are assumed as the physical circuit parameters of the converter systems. Otherwise, the population size and the learning rate need to be reset and updated. This threshold depends on the desired accuracy of the estimation results. It is worth noting that because the BA still has the challenge of locally optimal solutions, this problem can be avoided as much as possible by averaging through multiple calculations [29]. The setup of the multi-calculation times is discussed in Section V.

IV. Experimental Case Study

A. A developed plug-and-play carry-on test unit

To verify the proposed estimation method, a prototype unit is developed to perform the functions of signal generation and

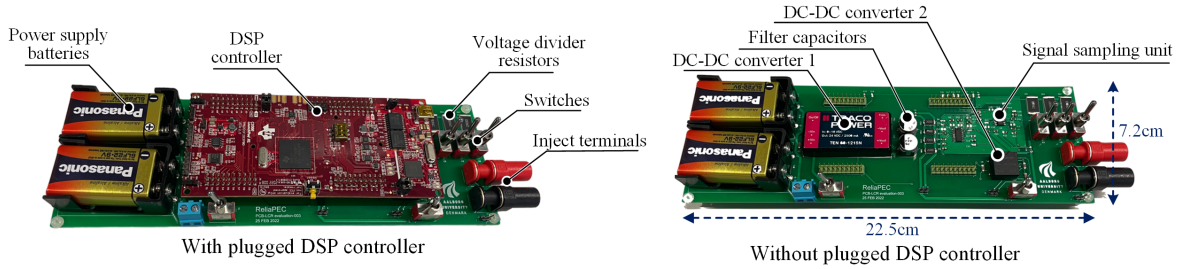

(a) Experimental prototype of the LC parameter characterization unit with signal injection and data measurement.

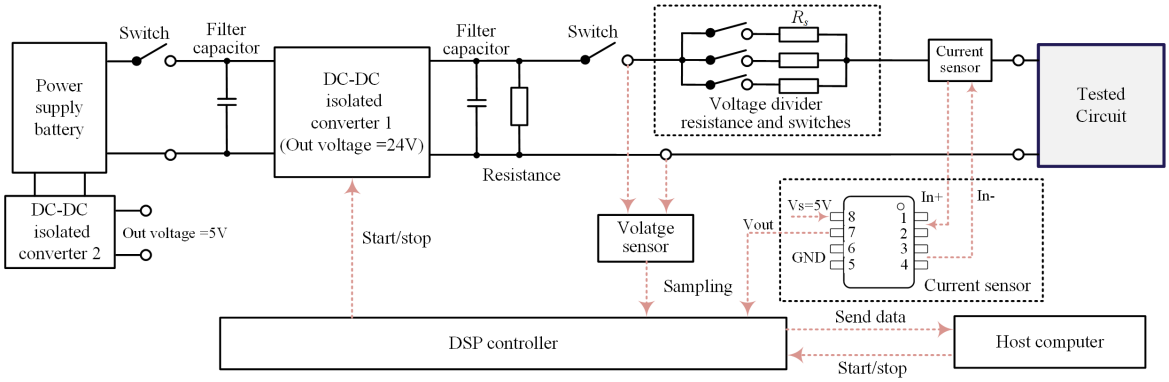

(b) Schematic diagram of the LC parameter characterization unit

Fig. 5. Experimental prototype and schematic diagram of the LC parameter characterization unit.

TABLE II
MEASURED VALUE OF LC PARAMETERS BY LCR METER IN TEST CASES.

C_1 (μF)							C_2 (μF)					L_1 (μH)	L_2 (μH)
2nd-order LC circuit network													
Case 1	Case 2	Case 3	Case 4	Case 5	Case 6	Case 7	-					Case 1 ~ Case 7	-
3197.4	2997.3	2801.3	2599.4	2398.4	2220.4	2009.4						4025.2	
3rd-order LC circuit network													
Case 8	Case 9	Case 10	Case 11	Case 12	Case 13	Case 14	Case 8 ~ Case 14					Case 8 ~ Case 14	-
3197.4	2997.3	2801.3	2599.4	2398.4	2220.4	2009.4	375.7					4025.2	
Case 15 ~ Case 19							Case 15	Case 16	Case 17	Case 18	Case 19	Case 15~ Case 19	-
2801.3							455.7	444.54	433.9	415.4	404.8	4025.2	
4th-order LC circuit network													
Case 20	Case 21	Case 22	Case 23	Case 24	Case 25	Case 26	Case 20 ~ Case 26					Case 20 ~ Case 26	Case 20 ~ Case 26
3197.4	2997.3	2801.3	2599.4	2398.4	2220.4	2009.4	375.7					4025.2	4151.8
Case 27 ~ Case 31							Case 27	Case 28	Case 29	Case 30	Case 31	Case 27 ~ Case 31	Case 27 ~ Case 31
2801.3							455.7	444.54	433.9	415.4	404.8	4025.2	4151.8

The value measured by the Keysight LCR meter E4980a (100Hz-25°C).

injection, and data collection and transmission, as shown in Fig. 5 (a). The signal is injected into the converter systems through the two terminals. It has a compact size and light weight, promising to be further developed as a hand-carry device for practical applications.

Fig. 5 (b) shows the schematic diagram of the developed test circuit. The test circuit is supplied with 18V by two batteries connected in series. The DC voltage component is fixed to 24 V based on the isolated DC-DC converter. And set several filter capacitors are connected in parallel at both terminals of the DC-DC converter and large resistance loads at the output ends of the DC signal generators to maintain the stability of the signal injection. The voltage divider resistors can be adjusted by selecting the toggle switches. The start and stop of the test circuit can be set through the host computer and the DSP controller. The sampled input current can be uploaded to the host computer through the sensors and DSP for follow-up algorithm analysis.

The TMCS1100A4 Hall current sensor is used to collect the current signal [31]. Firstly, the supply voltage V_s of the current sensor is 5 V, which is powered by the battery and a DC-DC converter. Then, the current sensor is connected in series with the test circuit, with the positive pole as In+ and the negative pole as In−. Since the measured current in this paper is positive, the reference voltage V_{ref} is set to 0 V, which is connected to ground terminal. Finally, the measured current corresponds to the output voltage V_{out}, which is collected in the DSP controller. In addition, to ensure the accuracy of sampling. After the current sensor is connected to the experimental unit, the current source is used to inject different current values to correct the bias and sampling ratio of the current sampling, to obtain accurate sampling current.

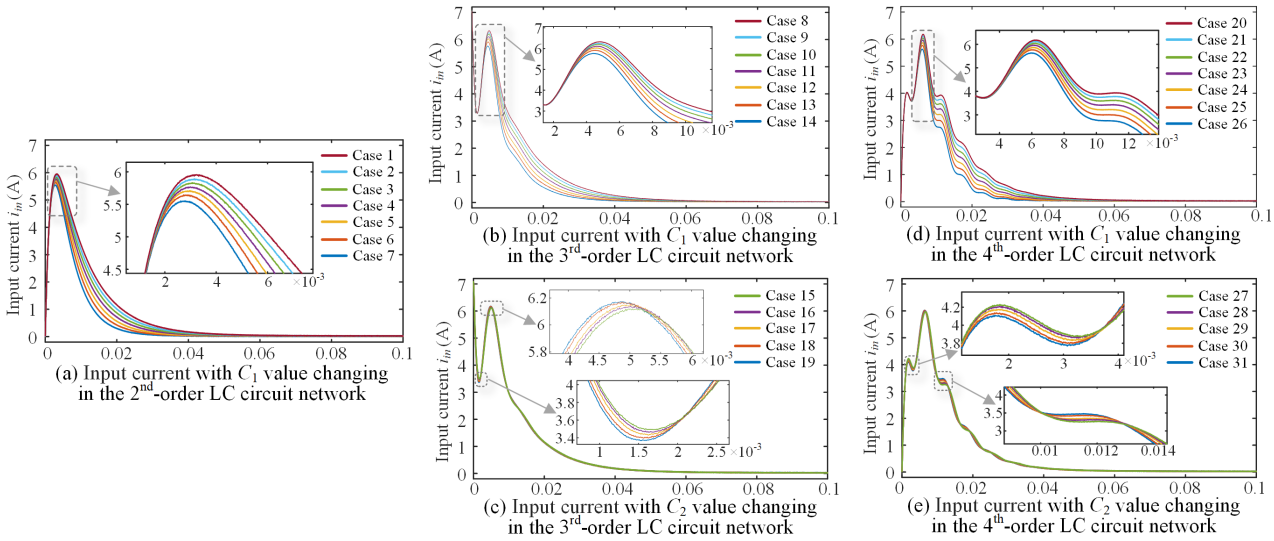

Fig. 6. Input current based on experimental tests. (Voltage dividing resistance R_s =3 Ω, sampling frequency: 10 kHz, the tested circuit parameters in different cases are given in Table II)

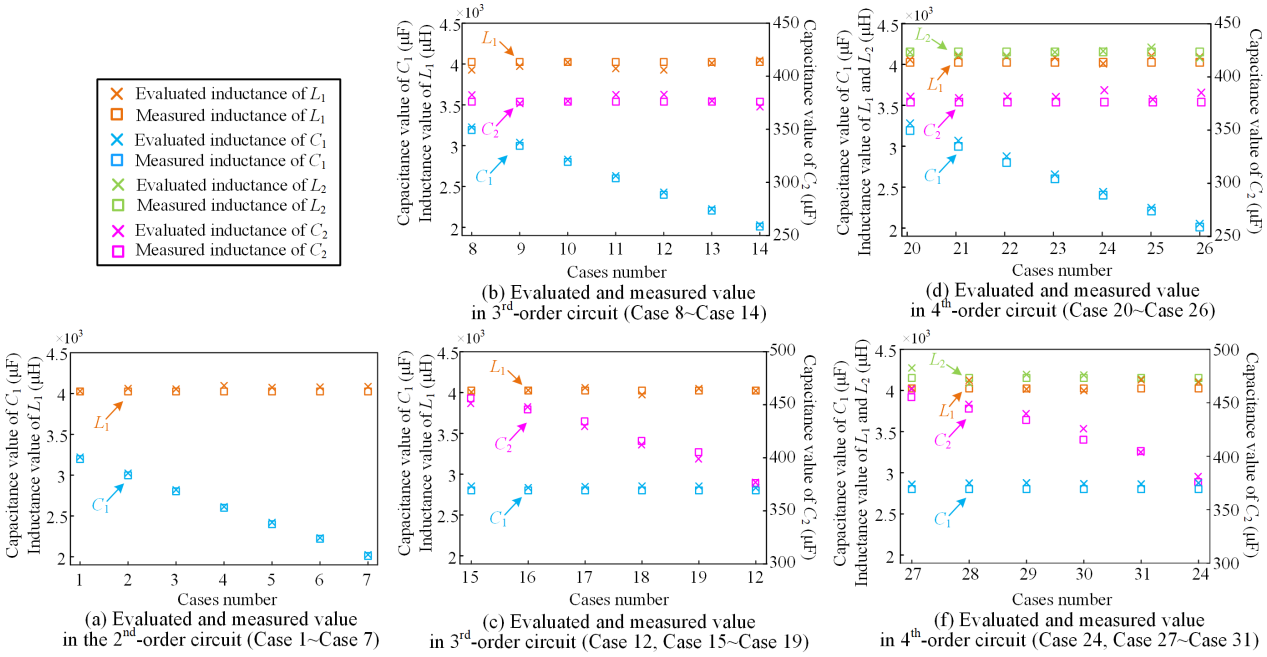

Fig. 7. Comparison of estimation and measurement values for LC parameters (The measurement values are given in Table II).

B. Testing and estimation results

The testing circuit consists of the converter system and LC components. The component selection and measured parameters are shown in Table II, which correspond to the 2^{nd}-order, 3^{rd}-order and 4^{th}-order LC circuit networks in Fig. 2, respectively. Case 1∼Case 7 belong to 2^{nd}-order tested circuits, Case 8∼Case 19 belong to 3^{rd}-order LC circuit networks, and Case 20∼Case 31 belong to 4^{th}-order LC circuit networks. To simulate the aging of the capacitor, the components C_1 and C_2 with different capacitances are configured.

Fig. 6 shows the injected current signals acquired for different cases, which are collected by the developed test unit. Fig. 6(a) shows the injected current signal when the tested circuit is a 2^{nd}-order LC circuit network, corresponding to the capacitance change of the C_1 (Case 1∼Case 7). Fig. 6(b) and (c) show the injected current signal when the tested circuit is a 3^{rd}-order LC circuit network, corresponding to the capacitance change of the C_1 (Case 8∼Case 14) and the capacitance change of the C_2 (Case 12, Case 15∼Case 19), respectively. Fig. 6(d) and (e) show the corresponding results when the tested circuit is a 4^{th}-order LC circuit network (Case 20∼Case 26). It can be seen that when the capacitance of C_1 and C_2 changes, the value of the input current also changes correspondingly. According to the estimation process in Fig. 4, the measured input current and the calculated input current are substituted into the optimization algorithm, thereby getting the estimation results of LC parameters.

The estimation and measurement values for LC parameters are compared and the results are given in Fig. 7, where the estimated value is the average value of 20 calculation times in

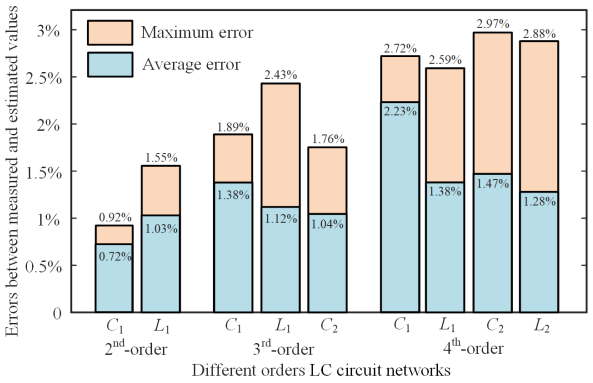

Fig. 8. Parameter estimation errors of LC parameters with different orders of LC circuit networks.

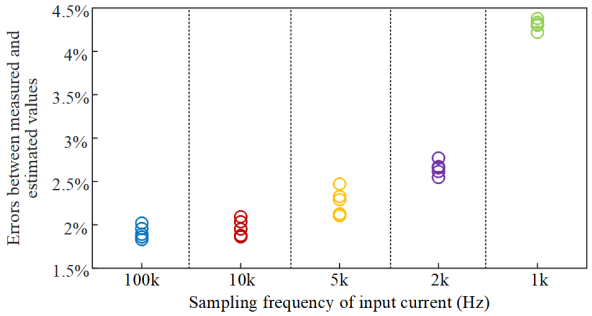

Fig. 9. Parameter estimation errors under different sampling frequency. (The error is the average error of the estimation results of L_1, L_2, C_1, and C_2; take Case 31 as the example.)

TABLE III
TESTING COMPARISON OF THE PROPOSED METHOD WITH EXISTING CONVERTER POWER-OFF STATE METHODS.

Method	Impact on the original system	Level of intrusion	Testing error		
			1st / 2nd order	3rd order	4th order
[15]	Need to additional current sensors for the original branch	+++	2.5%	Cannot be achieved	
[16]	Require additional blocking diodes for the PV panel	+++	1.5%		
[17]	Require intrusion into the controller to collect current and voltage signals	++	1.9%		
[18] [19]	Require intrusion into the original control system for setting the duty cycle	++	5.1%		
[20]	Need to intrusion into the original control system to turn on the IGBT module	++	2.1%		
Proposed method	No need to intrusion into the original control system, just using the carry-on unit in Fig. 5	+	1.55%	2.43%	2.97%

the algorithm. It can be seen from Fig. 7 (a) that the estimated capacitance of C_1 decreases correspondingly with the decrease of the actual capacitance, and it always maintains the same trend as the measured value. Similarly, in higher-order LC circuit networks, as the capacitances of C_1 and C_2 decrease, their estimation values decrease accordingly, as shown in Fig. 7 (b). It demonstrates that the test method can deal with the dynamic changes of parameters such as aging in the tested LC circuit networks.

Further, the errors in the estimation results are shown in Fig. 8. In the 2^{nd}-, 3^{rd}-, and 4^{th}-order LC circuit networks, the maximum errors of the capacitance estimation are 0.92%, 1.89%, and 2.97%, and the maximum errors of the inductance estimation are 1.55%, 1.76%, and 2.88%, respectively.

Table III gives the testing comparison of the proposed method with existing converter power-OFF state methods. Firstly, compared with existing methods, the proposed method does not require additional sensors and hardware components to be installed in the original system, and it also does not require intrusion into the original control system in converter power-OFF state. Therefore, the proposed method has the lower intrusion and testing risk level using the carry-on unit in Fig.5. In addition, when evaluating low-order circuits, the proposed method can still maintain low testing errors compared to existing methods. Furthermore, it is significant that the method proposed in this paper can achieve the parameter evaluation of high order equivalent circuits with 3rd and 4th-order, which is not possible with existing methods. Even for parameter evaluation of high-order circuits, the maximum test error of proposed method is still within 3%. Considering the parameter offset of inductors and capacitors is usually ±5%∼±20% in the datasheet, the method proposed in this paper can obtain more accurate parameter values by comparing the datasheets. In addition, the health condition of the parameters of the converter components can also be evaluated. For example, the failure standard of aluminum electrolytic capacitors is 20% drop in capacitance [14]. As the order of test circuits increases, the error of its estimation value also increases accordingly, which may be caused by the coupling effects of different parameters in high-order LC circuit networks.

V. DISCUSSION OF THE IMPLEMENTATION CONSIDERATIONS

A. Selection of injection resistance R_s

There are two requirements for the setup of injection resistance R_s: 1) The output current capability of the test unit is limited. Considering the potential short circuit condition of the LC circuit networks, the R_s should be greater than the ratio of the output voltage to the output current limit. 2) The R_s should be as small as possible after considering the limitation of the output capability of the test unit. For example, in the 2^{nd}-order circuit (3), when the R_s is large, the influence of the inductance L_1 is reduced. The sliding resistor is superior in performance for the application of this case, with appropriate power and current ratings, but has limitations in lightweight devices due to its large size and high cost. Therefore, considering the volume and cost, in the developed test unit, the value of different R_s can be configured through the combination of switches. In the actual testing, from a larger value to a smaller value of R_s can be applied to ensure the output of the test unit current and the accuracy of the estimation results.

B. Selection of sampling frequencies

It is significant to choose an appropriate sampling frequency for the current signal. The sampling frequency of the current signal affects the calculation time for the algorithm process

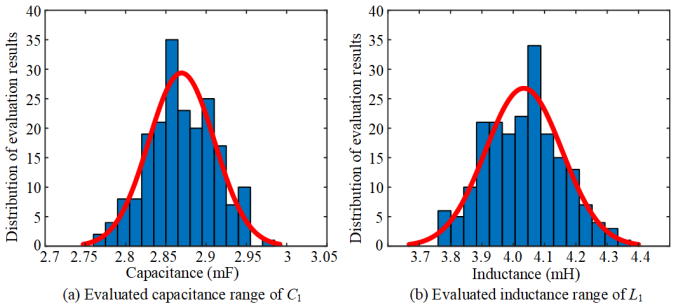

(a) Evaluated capacitance range of C_1 (b) Evaluated inductance range of L_1

Fig. 10. Distribution of estimation results. (Take the C_1 and L_1 in Case 31 as examples; Estimation results are calculated 200 times by the host computer.)

and the accuracy of the estimation results. Taking Case 31 in the 4^{th}-order LC circuit network as an example, the corresponding errors of current signals with different sampling frequencies are shown in Fig. 9, where the error represents the average error of the LC parameter estimation results. From the results, the accuracy of the estimation results increases when the sampling frequency is increased from 1 kHz to 10 kHz. When the sampling frequency is increased from 10 kHz to 100 kHz, the accuracy of the estimation results is almost the same. Therefore, the sampling frequency selection for this test method is 10 kHz.

C. Selection of the calculation times

Although the local optimal solutions frequently occur in swarm intelligence algorithms, this problem can be avoided as much as possible by averaging through multiple calculations. Taking Case 31 as an example, the estimation process is calculated 200 times by the host computer (each calculation takes about 40 seconds) to obtain 200 groups of parameter estimation results. Fig. 10 shows the distribution of the estimation results of C_1 and L_1, where the range of C_1 is [1.7∼3.4 mF], and the range of L_1 is [3.0∼4.5 mH] in the algorithm. It shows that the parameter estimation results are consistent with normally distributed. In this algorithm, a reasonable solution is obtained by calculating the average value of 20 times. However, it is worth noting that multiple solutions still cannot completely solve overcome the local optimal solution issue brought by the applied algorithm.

VI. Conclusion

This paper proposes an estimation method for LC circuits in power electronic converter applications, which can evaluate the internal LC parameters with 2^{nd}-order to 4^{th}-order in the converter systems without intruding into the original control system and circuit structures. The injection circuit with proper excitation is designed, the mathematical models of different circuit structures are developed, and an estimation algorithm to obtain the individual component parameters is proposed. A plug-and-play carry-on test unit is developed to provide the required DC voltage source and measure the current responses of the circuit network. With the selected voltage divider resistor (3 Ω), sampling frequency (10 kHz), and calculation times (20 times), the results show that the value of maximum parameter estimation errors is 1.5% for 2^{nd}-order circuit, 2.5% for 3^{rd}-order circuit, and 3% for 4^{th}-order circuit. It indicates that the proposed method achieves satisfactory estimation accuracy. The estimated parameter values of individual components can be further used for operation optimization and health condition monitoring in the converter systems.

References

[1] H. Wang, M. Liserre, and F. Blaabjerg, "Toward reliable power electronics: Challenges, design tools, and opportunities," *IEEE Ind. Electron. Mag.*, vol. 7, no. 2, pp. 17–26, Jun. 2013.

[2] Y. W. Li, "Control and resonance damping of voltage-source and current-source converters with LC filters," *IEEE Trans. Ind. Electron.*, vol. 56, no. 5, pp. 1511–1521, May. 2009.

[3] Y. Avenas, L. Dupont, N. Baker, H. Zara, and F. Barruel, "Condition monitoring: A decade of proposed techniques," *IEEE Ind. Electron. Mag.*, vol. 9, no. 4, pp. 22–36, Dec. 2015.

[4] S. Yang, D. Xiang, A. Bryant, P. Mawby, L. Ran, and P. Tavner, "Condition monitoring for device reliability in power electronic converters: A review," *IEEE Trans. Power Electron.*, vol. 25, no. 11, pp. 2734–2752, Nov. 2010.

[5] T. H. Nguyen and D.-C. Lee, "Deterioration monitoring of DC-link capacitors in AC machine drives by current injection," *IEEE Trans. Power Electron.*, vol. 30, no. 3, pp. 1126–1130, Mar. 2015.

[6] Z. Zhao, P. Davari, W. Lu, H. Wang, and F. Blaabjerg, "An overview of condition monitoring techniques for capacitors in DC-link applications," *IEEE Trans. Power Electron.*, vol. 36, no. 4, pp. 3692–3716, Apr. 2021.

[7] "Keysight technologies: Impedance measurement handbook." 4294A Precision Impedance Analyzer, https://www.keysight.com/us/en/assets/7018-06840/application-notes/5950-3000.pdf, 2019.

[8] K. Tsang and W. L. Chan, "Simple method for measuring the equivalent series inductance and resistance of electrolytic capacitors," *IET Power Electron.*, vol. 3, no. 4, pp. 465–471, Jul. 2010.

[9] A. M. R. Amaral and A. J. M. Cardoso, "An experimental technique for estimating the ESR and reactance intrinsic values of aluminum electrolytic capacitors," in *Proc. IEEE Instrum. Meas. Technol. Conf.*, 2006, pp. 1820–1825.

[10] A. M. R. Amaral and A. J. Marques Cardoso, "Simple experimental techniques to characterize capacitors in a wide range of frequencies and temperatures," *IEEE Trans. Instrum. Meas.*, vol. 59, no. 5, pp. 1258–1267, May 2010.

[11] T. Li, J. Chen, P. Cong, X. Dai, R. Qiu, and Z. Liu, "Online condition monitoring of DC-link capacitor for AC/DC/AC PWM converter," *IEEE Trans. Power Electron.*, vol. 37, no. 1, pp. 865–878, Jan. 2022.

[12] M. W. Ahmad, P. N. Kumar, A. Arya, and S. Anand, "Noninvasive technique for DC-link capacitance estimation in single-phase inverters," *IEEE Trans. Power Electron.*, vol. 33, no. 5, pp. 3693–3696, 2018.

[13] A. Wechsler, B. C. Mecrow, D. J. Atkinson, J. W. Bennett, and M. Benarous, "Condition monitoring of DC-link capacitors in aerospace drives," *IEEE Trans. Ind. Appl.*, vol. 48, no. 6, pp. 1866–1874, Nov.-Dec. 2012.

[14] H. Wang and F. Blaabjerg, "Reliability of capacitors for DC-link applications in power electronic converters—an overview," *IEEE Trans. Ind. Appl.*, vol. 50, no. 5, pp. 3569–3578, Sep./Oct. 2014.

[15] G. M. Buiatti, J. A. Martín-Ramos, A. M. R. Amaral, P. Dworakowski, and A. J. M. Cardoso, "Condition monitoring of metallized polypropylene film capacitors in railway power trains," *IEEE Trans. Instrum. Meas.*, vol. 58, no. 10, pp. 3796–3805, Oct. 2009.

[16] N. Agarwal, M. W. Ahmad, and S. Anand, "Quasi-online technique for health monitoring of capacitor in single-phase solar inverter," *IEEE Trans. Power Electron.*, vol. 33, no. 6, pp. 5283–5291, 2018.

[17] M. Kim, S.-K. Sul, and J. Lee, "Condition monitoring of DC-link capacitors in drive system for electric vehicles," in *IEEE Veh. Power Propulsion Conf.*, 2012, pp. 633–637.

[18] S. B. Lee, J. Yang, J. Hong, J.-Y. Yoo, B. Kim, K. Lee, J. Yun, M. Kim, K.-W. Lee, E. J. Wiedenbrug, and S. Nandi, "A new strategy for condition monitoring of adjustable speed induction machine drive systems," *IEEE Trans. Power Electron.*, vol. 26, no. 2, pp. 389–398, Feb. 2011.

[19] K.-W. Lee, M. Kim, J. Yoon, S. B. Lee, and J.-Y. Yoo, "Condition monitoring of dc-link electrolytic capacitors in adjustable-speed drives," *IEEE Trans. Ind. Appl.*, vol. 44, no. 5, pp. 1606–1613, 2008.

[20] H. Li, D. Xiang, X. Han, X. Zhong, and X. Yang, "High-accuracy capacitance monitoring of DC-link capacitor in VSI systems by LC resonance," *IEEE Trans. Power Electron.*, vol. 34, no. 12, pp. 12 200–12 211, Mar. 2019.
[21] D. Zhou, Y. Song, Y. Liu, and F. Blaabjerg, "Mission profile based reliability evaluation of capacitor banks in wind power converters," *IEEE Trans. Power Electron.*, vol. 34, no. 5, pp. 4665–4677, May 2019.
[22] A. Sangwongwanich, Y. Yang, D. Sera, and F. Blaabjerg, "Mission profile-oriented control for reliability and lifetime of photovoltaic inverters," *IEEE Trans. Ind. Appl.*, vol. 56, no. 1, pp. 601–610, Oct. 2020.
[23] B. Yao, X. Ge, D. Xie, S. Li, Y. Zhang, H. Wang, and H. Wang, "Electrothermal stress analysis and lifetime evaluation of DC-link capacitor banks in the railway traction drive system," *IEEE J. Emerg. Sel. Topics Power Electron.*, vol. 9, no. 4, pp. 4269–4284, Aug. 2021.
[24] H. Wen, W. Xiao, X. Wen, and P. Armstrong, "Analysis and evaluation of DC-link capacitors for high-power-density electric vehicle drive systems," *IEEE Trans. Veh. Technol.*, vol. 61, no. 7, pp. 2950–2964, Sep. 2012.
[25] J. S. Lim, C. Park, J. Han, and Y. I. Lee, "Robust tracking control of a three-phase DC–AC inverter for UPS applications," *IEEE Trans. Ind. Electron.*, vol. 61, no. 8, pp. 4142–4151, Aug. 2014.
[26] O. Husev, O. Matiushkin, D. Vinnikov, C. Roncero-Clemente, and S. Kouro, "Novel concept of solar converter with universal applicability for DC and AC microgrids," *IEEE Trans. Ind. Electron.*, vol. 69, no. 5, pp. 4329–4341, Jun. 2022.
[27] "Solve system of differential equations." Help Center for dsolve, https://www.mathworks.cn/help/symbolic/dsolve.html, 2022.
[28] X.-S. Yang, "A new metaheuristic bat-inspired algorithm," in *Nature inspired cooperative strategies for optimization (NICSO 2010)*. Germany: Springer, 2010, pp. 65–74.
[29] M. Beskirli and I. Koc, "A comparative study of improved bat algorithm and bat algorithm on numerical benchmarks," in *Proc. Int. Conf. Adv. Comput. Sci. Appl. Technol. (ACSAT)*, Dec. 2015, pp. 68–73.
[30] Y. Peng, S. Zhao, and H. Wang, "A digital twin based estimation method for health indicators of DC–DC converters," *IEEE Trans. Power Electron.*, vol. 36, no. 2, pp. 2105–2118, Feb. 2021.
[31] "TMCS1100 precision isolated current sensor with external reference." Texas Instruments, https://www.ti.com/document-viewer/TMCS1100/datasheet/GUID-EF0EA45E-9AA6-4086-BE0B-5671FAE79DEE#TITLE-SBOS820SBOS8209912, 2021.

Bo Yao (Student Member, IEEE) received the B.Eng. and M.Eng. degrees in electrical engineering from Southwest Jiaotong University (SWJTU), Chengdu, China, in 2017 and 2020, respectively.

He is currently working toward the Ph.D. degree in power electronic with Aalborg University, Aalborg, Denmark. He is also currently a research assistant at the Energy Department of Aalborg University in cooperation with Vestas Wind Systems A/S. His research interests include reliability evaluation and condition monitoring of power electronic components in power converter systems.

Mr. Yao was a recipient of the Best Paper Award of International Conference on Electrical Machines and Systems (ICEMS) in 2019, and the SEMIKRON Young Engineer Award from the ECPE European Center for Power Electronics and SEMIKRON Foundation in 2023.

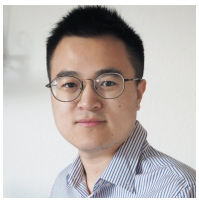

Yingzhou Peng (Member, IEEE) received the B.S. degree in electrical engineering from Harbin Engineering University, Harbin, China, in 2014, the M.S. degree in power electronics from Chongqing University, Chongqing, China, in 2017, and the Ph.D. degree in power electronics from Aalborg University, Aalborg, Denmark in 2020. From 2020 to 2022, He was a PosDoc with Aalborg University, Aalborg, Denmark. He was a Visiting Researcher with the Electrical Power and Energy Conversion Lab, Cambridge University, U.K, in 2020. He is currently working as an Assistant Professor at Hunan Unversity, China.

His research interests include the failure mechanisms analysis of power electronic components, the improvement of the robustness and reliability of power converters by means of condition monitoring.

Yichi Zhang (Student Member, IEEE) received the B.Eng. degree in electrical engineering from Shenyang Agricultural University (SYAU), Shenyang, China, in 2017, the M.S. degree in power electronics from Southwest Jiaotong University (SWJTU), Chengdu, China, in 2021.

He is currently working toward the Ph.D. degree in power electronic with Aalborg University, Aalborg, Denmark. His research interest is the thermal evaluation and condition monitoring of semiconductor devices in power electronic systems.

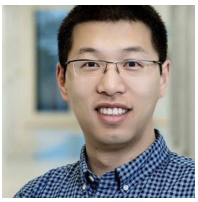

Haoran Wang (Member, IEEE) received the B.S. and M.S. degrees in control science and engineering from the Wuhan University of Technology, Wuhan, China, in 2012 and 2015, respectively, and the Ph.D. degree in energy technology from the Center of Reliable Power Electronics, Aalborg University, Aalborg, Denmark, in 2018.

From 2013 to 2014, he was Research Assistant with the Department of Electrical Engineering, Tsinghua University, Beijing, China. He was a Visiting Scientist with the ETH Zurich, Zurich, Switzerland, from 2017 to 2018, with Kiel University, Kiel, Germany, and Danfoss Drives A/S, Denmark, in 2019. From 2019 to 2021, he was an Assistant Professor with Aalborg University, Aalborg, Denmark. Currently, he is the Vice General Manager with Three Gorges Intelligent Industrial Control Technology Company Ltd., Yichang, China. His research interests include reliability of electrical and electronic components and systems, multiobjective life-cycle performance optimization of power electronic systems, and reliable clean energy control systems.

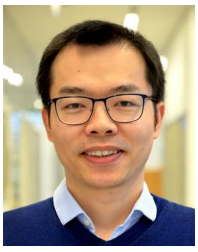

Huai Wang (Senior Member, IEEE) received the B.E. degree in electrical engineering from the Huazhong University of Science and Technology, Wuhan, China, in 2007, and the Ph.D. degree in power electronics from the City University of Hong Kong, Hong Kong, in 2012.

He is currently a Professor with AAU Energy, Aalborg University, Aalborg, Denmark, where he leads the Group of Reliability of Power Electronic Converters (ReliaPEC) and the mission on Digital Transformation and AI. He was a Visiting Scientist with ETH Zurich, Switzerland, from August to September 2014, and with the Massachusetts Institute of Technology, Cambridge, MA, USA, from September to November 2013. He was with the ABB Corporate Research Center, Switzerland in 2009. His research interests include the fundamental challenges in modeling and validation of power electronic component failure mechanisms and application issues in system-level predictability, condition monitoring, circuit architecture, and robustness design.

Dr. Wang was the recipient of the Richard M. Bass Outstanding Young Power Electronics Engineer Award from the IEEE Power Electronics Society, in 2016, and the 1st Prize Paper Award from IEEE TRANSACTIONS ON POWER ELECTRONICS, in 2021. He serves as an Associate Editor for the Journal of Emerging and Selected Topics in Power Electronics and IEEE TRANSACTIONS ON POWER ELECTRONICS.